A U-Shape Fibre-Optic pH Sensor Based on Hydrogen Bonding of Ethyl Cellulose With a Sol-Gel Matrix

Zijuan Tang, David Gomez, Chenyang He, Serhiy Korposh, Stephen P. Morgan, Ricardo Correia, Barrie Hayes-Gill, Kerry Setchfield, and Liangliang Liu

***Abstract*—Development of a biocompatible pH sensor is of importance in biomedical applications, particularly for in vivo measurement, providing necessary information for clinical diagnosis and treatment such as chronic wounds and foetal acidosis. Traditional pH-indicator based optical sensors have problems of dye-leaching and photobleaching that restrict their uses in long-term monitoring. In this work, a dye-free fibre optic pH sensor is proposed consisting of a U-shape multimode optical fibre coated with a hybrid organic-inorganic composite film. The film is formed by cross-linking ethyl cellulose with a silica matrix at an optimised ethyl cellulose/silica molar ratio of 0.0065 via weakly interacted hydrogen bonding. This bonding is affected by hydrogen concentration (i.e., pH) in a solution resulting in a morphological change of the polymer aggregation presented in the silica matrix leading to refractive index change of the film. The developed sensor shows a reversible response to pH from 4.5 to 12.5 and exhibits linear correlation between transmitted light power and pH with a limit of agreement (LoA) between the sensor and a commercial probe of ±0.2 pH. For a clinically important range of pH values between 6 and 8 the LoA is ±0.1 pH. The sensor has low cross-sensitivity to temperature as the maximum interpreted pH change attributed to the power change is 0.12 pH when the temperature changes from 21 °C to 39 °C. To demonstrate biomedical relevance, the sensor is used to monitor pH of human serum. An in-house cytotoxicity assay is conducted with mouse fibroblast cell revealing that the film is not cytotoxic.**

***Index Terms*—pH optical sensor, dye-free, ethyl cellulose sol-gel film, cytotoxicity assay.**

Manuscript received July 11, 2020; revised September 11, 2020 and October 20, 2020; accepted October 26, 2020. Date of publication October 28, 2020; date of current version March 1, 2021. This work was supported by the Medical Research Council under Grant U.K., MR/R025266/1. The work of Zijuan Tang was supported by the China Scholarship Council. *(Corresponding author: Liangliang Liu.)*

Liangliang Liu is with the Optics and Photonics Group, Faculty of Engineering, University of Nottingham, Nottingham NG7 2RD, U.K. (e-mail: liangliang.liu1@nottingham.ac.uk).

Zijuan Tang is with the School of Electronic and Information Engineering, Beijing Jiaotong University, No. 3 Shangyauncun, Haidian District, Beijing 100044, China (e-mail: 17111024@bjtu.edu.cn).

David Gomez, Chenyang He, Serhiy Korposh, Stephen P. Morgan, Ricardo Correia, Barrie Hayes-Gill, and Kerry Setchfield are with the Optics and Photonics Group, Faculty of Engineering, University of Nottingham, Nottingham NG7 2RD, U.K. (e-mail: ezzdg3@exmail.nottingham.ac.uk; eexch9@exmail.nottingham.ac.uk; ezzsk2@exmail.nottingham.ac.uk; eezspm@exmail.nottingham.ac.uk; ricardo.goncalvescorreia@nottingham.ac.uk; eezbrhg@exmail.nottingham.ac.uk; plzks1@exmail.nottingham.ac.uk).

This article has supplementary downloadable material available at https://ieeexplore.ieee.org, provided by the authors.

Color versions of one or more of the figures in this article are available online at https://ieeexplore.ieee.org.

Digital Object Identifier 10.1109/JLT.2020.3034563

I. Introduction

ACCURATE pH monitoring plays a vital role in many fields such as environmental monitoring, wastewater treatment, food industries, clinical diagnosis and treatment [1]–[3]. In the field of biomedicine, there is great demand for real-time and accurate pH measurement. For example, in vitro cell culture needs to be in the range of 6.5 to 7.7 as cell growth is diminished when the buffer pH is outside this range [4]. For chronic wounds such as diabetic foot ulcers, monitoring changes in wound exudate pH can indicate healing rate or infection with early intervention helping to reduce economic costs [5]. Active movement of tumour cells is an essential process of malignant proliferation, which will increase if the extracellular pH is moderately acidic (≈6.7) [6]. Foetal acidosis is commonly defined as a low umbilical pH, or a high umbilical base deficit. When defined by a low umbilical pH (with threshold for cut-off varying between 7.2 and 7.0), acidosis is associated with neonatal morbidity and mortality [7].

Currently, most commercially available pH sensors measure the potential difference between two glass electrodes and can obtain a pH detection range of 0–14 and a resolution of 0.01 pH. However, such electrochemical sensors generally have bulky size that makes them not applicable to samples of small volume. Optical fibre sensors (OFS), owing to their advantages including miniaturisation, multiplexing, capability of remote sensing and high versatility have drawn research interests in developing sensing devices in the field of biomedical applications [8]–[10]. Importantly they can be easily integrated into existing medical devices such as wound dressings, foetal scalp electrodes or biopsy needles for real-time diagnosis or prognosis. A variety of pH OFSs based on different sensing mechanisms have been developed. OFSs based on fluorescent compounds or indicator dyes typically measure pH by monitoring optical signals such as absorption, fluorescence intensity or life-time [11]–[14]. Despite high sensitivity, these types of sensors typically suffer from problems such as dye-leaching and photobleaching that cause a reduction in the sensitivity and long-term stability [15].

To overcome these problems, there is considerable interest in developing dye-free OFSs for monitoring pH via measurement of the refractive index or the mechanical property of a pH-sensitive film. For example, Cheng *et al*. reported a polymer fibre Bragg grating (FBG) sensor in which pH is determined

via monitoring strain induced by swelling of a pH-sensitive hydrogel film deposited on the FBG achieving a sensitivity of −0.41 nm/pH for pH = 3–6.5 [16]. Aldaba *et al*. reported polyaniline coated tilted FBG sensor which measured pH via a change of refractive index (RI) of the polyaniline film and the achieved sensitivity higher than 30 pm/pH for pH = 2–12 [17]. A surface plasmon resonance (SPR) based optical fibre pH sensor is reported by Semwal *et al*. which is functionalised with a reduced graphene oxide-polyaniline (rGO-Pani) nanocomposite layer whose refractive index changes with pH. With this design, a peak sensitivity of 75.09 nm/pH and a response range of 2.4 to 11.35 are obtained [18]. Although these sensors show promising results in measuring pH, the fabrication process requires specific expensive facilities such as a high-power laser for grating based sensors or thin film coating device for SPR sensors that are not easily accessible. They also require interrogators such as a tuneable laser system that can be expensive for clinical application. Therefore, to achieve widespread use of this technology, it is beneficial to develop intensity-based sensors that can be monitored using low cost instrumentation.

The sol-gel technique is one of the popular methods to encapsulate and immobilise pH-sensitive materials such as dye compounds on an OFS [19], [20]. The resulting three-dimensional matrix has high stability, porosity and surface area, which are beneficial to the diffusion of ions in solution for measuring pH [21], [22]. Cellulose is the most produced organic polymer and approximately 5×10^{11} metric tons are generated each year [23]. It possesses promising properties including biocompatibility, high sorption capacity, relative thermostability and changeable optical appearance that are beneficial for the design of an optical sensor [24]. All optical based chemical sensors reported so far with cellulose, to the best of our knowledge, deploy cellulose as a matrix film for encapsulating or binding sensing elements for detecting parameters such as gases [25] and pH [26]. For example, Chu *et al*. reported a fluorescence pH sensor involving doping CdSe/ZnS quantum dots in an ethyl cellulose (EC) matrix for sensing of pH. The determination of pH relies on the fluorescent intensity of the quantum dots while the ethyl cellulose is the matrix film and does not participate in sensing pH [27]. The sensing property of EC for a specific parameter such as pH has not been studied previously.

A U-shape OFS is a popular platform for measuring pH due to its extended evanescent field in pH sensitive films leading to an increase of interactions between light and pH indicators [28], [29]. In this work, a dye-free U-shape fibre-optic pH sensor is reported with an organic-inorganic composite film that contains ethyl cellulose and silica prepared via a sol-gel reaction. To the best of our knowledge, the composite film reported in this work is used for pH sensing for the first time. Results indicate that EC can be used to measure pH via a change of aggregation states within a silica film. The sensor reveals high sensitivity and reversibility to pH over a wide tested range (4.5 to 12.5), and low temperature cross-sensitivity in the range (21 °C to 39 °C). As the ultimate application is in healthcare, an in-vitro test with mouse fibroblast cells is used to evaluate the cytotoxicity of the film.

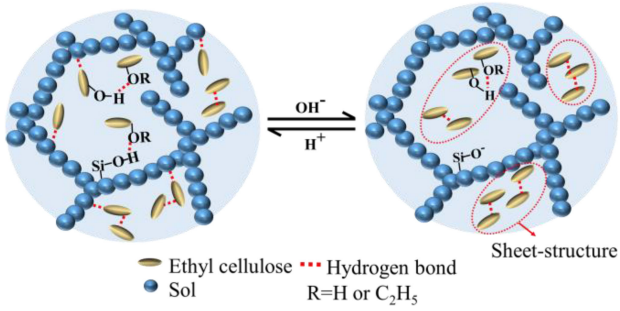

Fig. 1. Schematic illustration of the pH response of the film: hydrogen bonding of EC to silica matrix at lower pH (L) and sheet-structure of EC in a higher pH (R).

II. Method

A. Sensing Mechanisms

1) Composite Coating: A pH sensing film is prepared through a sol-gel reaction with co-embedding of EC polymer. TEOS (tetraethyl orthosilicate) undergoes hydrolysis and polycondensation under the catalysis of HCl, resulting in a network structure of sols with silanol groups (Si-OH) terminated (Fig. 1). EC contains hydroxyl (-OH) and ethoxy groups ($-OC_2H_5$) on polymer chains that form hydrogen bonding with Si-OH in the sol-gel matrix. On the other hand, due to the hydrophobic properties of the glucopyranose plane, the cellulose chain can stack via hydrophobic interaction and form a sheet-like structure [30]. Therefore, the EC polymer bears two types of molecular forces (hydrogen bonding and hydrophobic force) and its aggregation state is affected by these two forces. The hydrophobic force tends to shape EC into a sheet-like structure whereas the hydrogen bonding competes with the hydrophobic force to break the sheet-like structure (illustrated in Fig. 1). A solid porous structure with a silica/EC hybrid film is finally produced with an annealing process at 70 °C for 48h.

The weakly interacted hydrogen bonding is reversibly interrupted by protonation/deprotonation of Si-OH in different pH solutions (Fig. 1). Thus, the EC polymers inside the silica film undergo morphological changes with loosening or tightening of polymer chains under the two competing forces leading to a change of the refractive index.

2) U-Shape Optical Fibre Sensor: The schematic diagram of the produced U-shape sensor is shown in Fig. 2a where the pH-sensitive film with refractive index n_2 is deposited on the bare region of the U-bend. A longitudinal-section and cross-section view of the curved portion is shown in Fig. 2b, and Fig. 2c. The input power P_i is the intensity value of a particular wavelength λ of a straight fiber with the same length of the sensor and the output power P_o is the intensity value of the U-shape pH sensor in a solution at a specific pH value. P_o can be calculated as a function of P_i in Eq. (1) according to the model analysis of multiple reflection losses of light in a bent fibre [31].

$$P_o = P_i \int_0^{\rho} r dr \int_0^{2\pi} d\psi \int_0^{\alpha_c} \cos\theta \cdot \sin\theta d\theta \int_0^{2\pi} d\phi \exp[-\gamma \cdot \xi] \quad (1)$$

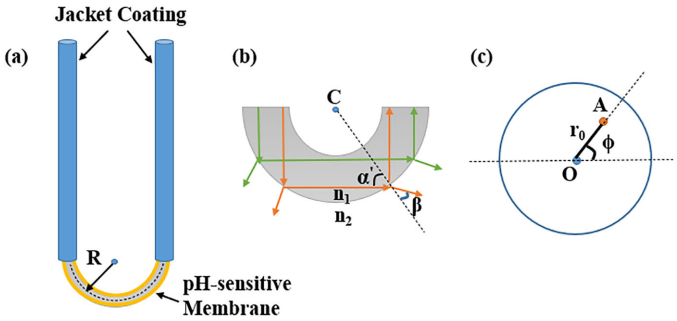

Fig. 2. (a) Schematic of the proposed U-shaped sensor, where the bare region with a radius R is coated with the pH-sensitive film. (b) Longitudinal cross-section image of the bare region. α' and β are the incidence angle and refraction angle of a ray on the core-film interface, respectively. n_1 and n_2 represent the refractive index of the core and film. (c) Cross-section image of the bare fibre. r_0 and ϕ are the rotation angle and distance between the incident point A and the origin O on the cross section of the optical fibre.

where ρ is the core radius of the fibre; α_c is the complementary critical angle and is given by $\cos\alpha_c = n_2/n_1$; ξ is the curvature length and $\xi = \pi R$; Eq. (1) describes power output of a bend fibre which splits the bend region into a series of small sections, the γ represents summation of the transmission coefficient of the ray at all reflection point per unit length of fibre, γ is therefore can be given by [32]

$$\gamma = \frac{k\lambda n_2 \sin\alpha \tan\alpha}{2\pi\rho {n_1}^2 \sin^2\alpha_c (\cos^2\alpha - \cos^2\alpha_c)^{1/2}} \tag{2}$$

where α is the angle between incident ray and the core axis and it is the complementary angle of the incident angle α'. k is the bulk absorption coefficient of the film, which is constant and independent of pH change as seen in Figure S.3 (supplementary material). The correlation of attenuation coefficient to the refractive index n_2 has plotted from Eq. (2) and is shown in Figure S.1 in supplementary material. In addition, the power output from a bare U-shape fibre has been measured experimentally for different refractive index media (Figure S.2) which further confirms this response. This indicates that the attenuation coefficient increases as n_2 increase, and as a result the output power decreases correspondingly. Therefore, by monitoring the output power change of the transmission spectrum, the pH value that modulates n_2 can be obtained.

The sensitivity of the U-shape sensor, defined as power change per unit of the analyte, decreases with increase of curvature radius according to Eq. (1). A thorough theoretical simulation of the U-shape OFS can be found in a recent publication by Danny *et al*. [33]. It demonstrates that the optimal sensitivity of such sensors can be obtained when the bending ratio, defined as the ratio of bending radius to fibre radius is less than 17. The bending ratio of the proposed U-shape sensor is 15, thus it is considered to be operating under optimal conditions.

B. Sensor Fabrication

1) Preparation of the pH-Sensitive Film: The preparation process of the pH-sensitive membrane used in the experiment is as follows:

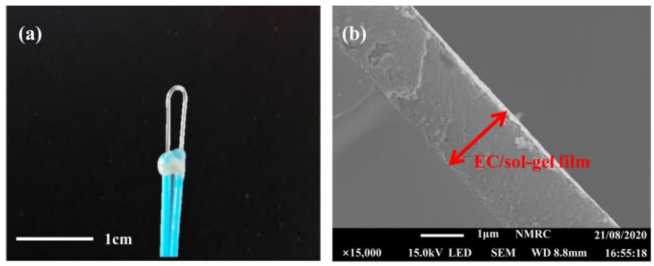

Fig. 3. (a) The fabricated U-shape sensor. (b) Cross-section of the film observed under SEM.

1) 266 mg of EC (48% ethoxyl, Sigma-Aldrich, UK) is dissolved in 40 mL of N, N-Dimethylformamide (DMF, 99.8%, 0.944 g/mL, Sigma-Aldrich, UK), followed by stirring overnight.
2) The sol-gel precursor is prepared by mixing 2 mL of TEOS (98%, 0.933 g/mL, Sigma-Aldrich, UK), 4 mL of pure ethanol, 675 μL of deionised water, 50 μL of HCl (37%, 1.179g/mL, Sigma-Aldrich, UK) in a 20 ml volume vial under stirring at 50 °C for 10 min. The molar ratio of TEOS to water is 1:4 to ensure that TEOS is completely hydrolysed. The volume ratio of TEOS to Ethanol is 1:2, which helps to prevent immobilising the hydrolysis reaction while dissolving TEOS [34].
3) The dissolved polymer in step (1) is mixed with the sol-gel precursor prepared in step (2) with a volume ratio of 0%, 25%, 40%, 60%, 75%, 100%. The corresponding molar ratios of EC/Silica are 0, 0.0033, 0.0065, 0.015, 0.029 and pure EC, where the chemical amount of TEOS is equal to that of Silica after hydrolysis and polycondensation of TEOS.
4) All the mixed solutions obtained in step (3) are stirred at 50 °C on a magnetic stirrer for 1h and then stirred overnight at room temperature.

2) U-Shape Sensor Fabrication Procedure: A 40 cm long hard-clad multimode optical fibre (core: Ø200 μm, NA: 0.39, Thorlabs, UK) is folded from its centre to a fixed radius. Two symmetric points away from the centre (~2 cm) on the two arms are fixed to ensure the fibre bears the same level of stress to enable the formation of a sharp bend during fabrication. A ~2 cm long region of the polymer cladding in the central area is removed completely by flame. As the flame temperature (~1430 °C) is higher than the softening point (1032°C) of silica fiber [35], the silica fibre is softened at the centre and reshaped into a relatively small radius (1.5 mm) U-shape under stress and the stress is then released during heating. The U-shape is permanently formed after cooling. A series of U-shape sensors with equal length and almost uniform bending radius of 1.5 ± 0.2 mm are fabricated in the same way. Fig. 3a shows one of the fabricated U-shape sensors. A dip-coating method is subsequently adopted to coat the U-shape region with the prepared coating solution with a coating speed of 9 mm/s by using an automatic dip coating machine (HO-TH-02, Holmarc, India). Finally, the coated sensors are annealed in an oven at a temperature of 70 °C for 48h to remove the solvent and stabilise

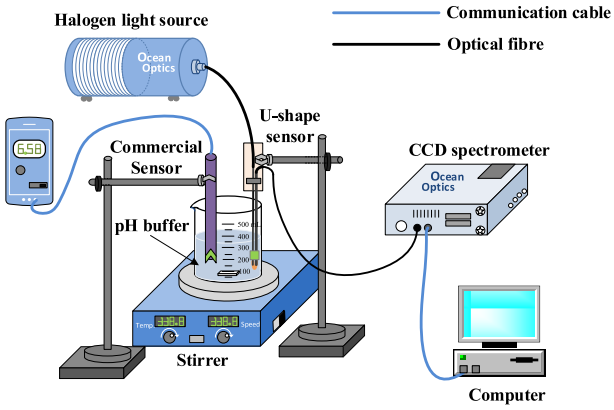

Fig. 4. Schematic diagram of the experimental set-up for pH measurement. Both sensing probes of the U-shape sensor and commercial electrochemical sensor are dipped into buffer solution and the beaker containing the buffer was placed on a magnetic stirrer to keep stirring. The input light from the light source enters the U-bend fibre and is detected by a spectrometer and in turn to a computer.

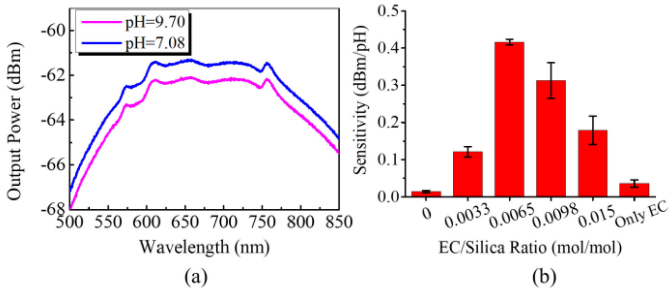

Fig. 5. (a) The transmission spectrum of the sensor with an EC/Silica molar ratio of 0.0065 at pH 7 and 9.7. (b) pH sensitivities of 6 U-shape sensors with different EC/Silica molar ratios, error bars represent the variation of 5 repeated measurements of each sensor.

the film. The thickness of the film measured by SEM is 1.71 μm as shown in Fig. 3b.

C. Cytotoxicity Testing

The cytotoxicity assays of the film are conducted via direct contact method and elution method respectively using mouse fibroblast cells. The former is to culture the cells in direct contact with the film and the latter is to culture cells with the film elution solutions. After culture period of 24h and 72h, neutral red cell cytotoxicity assays were carried out to estimate the cell viability. The detailed testing process is given in the supplementary materials.

D. Experimental Set-Up and Procedure

The schematic of the experimental set-up for pH measurement is shown in Fig. 4. A halogen light source (HL-2000, Ocean Optics, UK) is used to provide incident light for the sensor. The optical fibre is fixed on a lab-frame with the U-shape sensing region totally immersed in a Tris buffer solution (0.01M, pH = 6.4). Magnetic stirring is applied to ensure ions diffuse quickly while adjusting the pH of the solution. A commercial electrochemical pH sensor (PHH-37, OMEGA, USA) is also immersed in the buffer solution to provide a pH reference in real-time. The transmission spectra are detected by a CCD spectrometer (USB 2000, Ocean Optics, UK), which is connected to a computer for data processing.

For sensor calibration, the pH of the buffer solution is adjusted in steps with an interval of ~1 between the range of pH = 4.5 to 12.5 via adding NaOH/HCL into the buffer solution. Each step is held for at least 5 min to ensure the response of the OFS has stabilised. Both signals from pH meter and OFS are sampled at 1 Hz.

A temperature cross-sensitivity test is performed by utilising a thermostatic water bath filled with deionised water (stability: ± 0.2 °C, Grant Aqua Plus, UK). The temperature is programmed in increments with steps from 21 °C to 39 °C and the spectral response of the sensor is monitored at a frequency of 1 Hz. Each temperature step is measured for 10 min to ensure that the response of the OFS has stabilised.

An in vitro test of pH monitoring in human serum is carried out by placing the calibrated sensor in human serum with a volume of 1 ml. The pH of the serum is adjusted from 7.7 to 6.4 by titrating with HCl solution. pH paper strips are used for indicating pH before and after where the commercial pH probe used previously failed to apply due to the small volume of sample making it unsuitable for the commercial electrochemical pH sensor.

III. Experimental Results

A. Sensor Optimisation

As introduced in Section II, the sensing of pH relies on the weak interaction of EC with silica matrix, the molar ratio of the two presented in the final film determines the pH sensitivity. In order to investigate the optimal sensitivity, 6 U-shape sensors were prepared by coating with different coating solutions with different EC/Silica molar ratio. Fig. 5a shows the spectral response of the sensor with the EC/Silica molar ratio of 0.0065, demonstrating that the overall power of the transmission spectrum decreases as pH increases from 7 to 9.7. The biggest change of the power is located around 609 nm, thus the average power between 608–610 nm is used for reporting dynamic pH response of the OFS in the following content. Fig. 5b shows the sensitivity comparison of different sensors fabricated with different EC/Silica molar ratios for the pH range between 7 and 10. As the molar ratio increases, the pH sensitivity of the sensor increases and then decreases. The highest sensitivity can be obtained when the molar ratio is 0.0065. Thus, this ratio of EC/Silica film is adopted for all subsequent experimental measurements. In addition, the sensor exhibits extremely low sensitivity when there is only EC or only sol-gel, indicating that silica or the EC film alone is not pH-sensitive.

Fig. 6a shows an SEM image of the pH-sensitive film that indicates the uniformity of the film. The element mapping of the film is obtained via energy-dispersive X-ray spectroscopy (EDS) and Fig. 6b shows the mass fraction of the elements (C and Si) from EDS analysis of films with different EC/Silica molar ratios. The result shows that the mass fraction of C and Si increases and

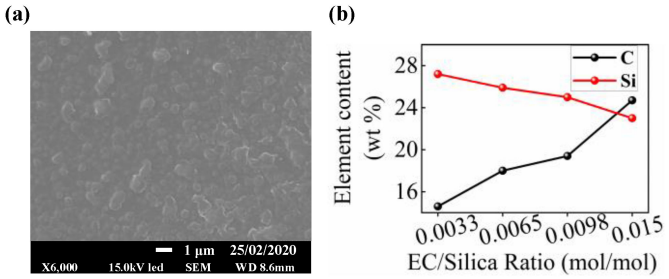

Fig. 6. (a) SEM image of the EC/Silica film, scale bar = 1 μm; (b) The content of C and Si elements in films with different EC / Silica molar ratios from EDS analysis.

decreases respectively as the increase of EC. The Si and of C elements are from silica and EC, respectively.

B. pH Measurement With OFS

The spectral response of the developed U-shape sensor in air and in different pH solutions is shown in Fig. 7a by using experimental set-up shown in Fig. 4 with an enlarged spectrum at around 609 nm inserted on the right-hand side. The temperature, monitored in real-time with the thermometer embedded inside the pH electrode, remains relatively stable at 22 ± 0.5 °C. The spectra in Fig. 7a demonstrate that the overall power of the transmission spectrum increases as pH decreases from 4.5 to 12.5. This indicates that the refractive index of the film increases with an increase of pH that is referenced by an experimental measurement of refractive index sensitivity from a U-shape fibre sensor in Figure S.2. The decrease of pH promotes formation of hydrogen bonding as a result of protonation of the silanol groups. Consequently, the EC polymers spread and bond to the silica matrix. Fig. 7b shows a linear fitting of the output power as a function of pH. Two distinct sensitivities are present with a sensitivity of −0.42 ± 0.02 dBm/pH in the range of 7.5–12.5 and −0.14 ± 0.01 dBm/pH in the range of 4.5–7.5. The reverse trace when pH decreases from 12.5 to 4.5 matches well to its increase, indicating good reversibility of the sensor to pH and absence of hysteresis. Taking into account that the resolution of the spectrometer, the pH resolution of the developed U-shape sensor is then determined as 0.02 ± 0.002 pH. The sensitivity of the sensor decreases to about half of their initial values when the pH value is lower than 7.5. This is associated with the acid dissociation constant (pKa) of the silanol groups, reported as pKa = 8.5 when they are in-plane [36]. When pH is less than 8.5, more unprotonated silanol groups are protonated and hydrogen bonding forces start to dominate. The sheet-like structure of EC polymer induced by hydrophobic force may have completely disassembled and moved to another phase of reorganisation due to hydrogen bonding. The limit of agreement (LoA) of the U-shape sensor compared to the commercial sensor in pH measurement is calculated as ±0.2 pH over the range of 4.5–12.5 and ±0.1 pH over the range of 6–8 based on Bland-Altman analysis (Figure S.4 in supplementary file). Fig. 7c shows the dynamic response of the U-shape sensor to pH and the output power shows apparent step changes in response to pH variation between 4.5 and 12.5. The response time of the sensor is obtained

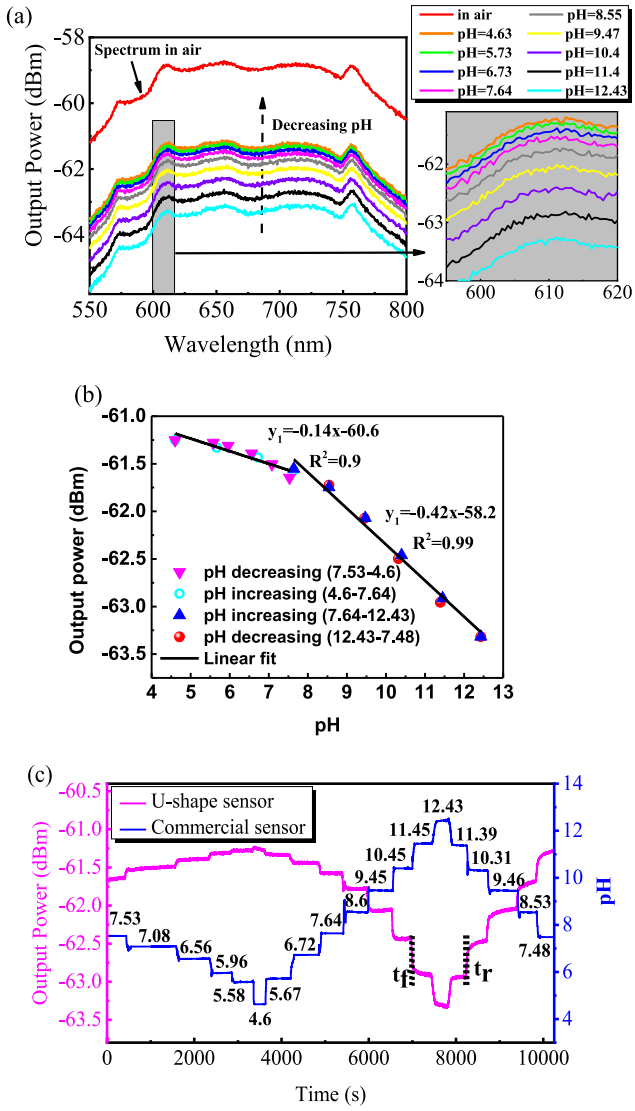

Fig. 7. (a) The spectral response of the U-shape sensor to pH; (b) linear fitting of average output power (608–610 nm) as a function of pH. Error bars are smaller than marker size; (c) dynamic response of the power to pH and response time measurement.

in terms of 90% power change between two pH and the results show the average rise and fall times of the sensor are 45 and 46.6 s, respectively.

C. Temperature Response

Temperature cross-sensitivity is a common issue for polymer based optical sensors due to potential thermal expansion of polymers and silica fibre, which may cause a change of refractive index (n_1 and n_2) and affect the stability of output power. In addition, when the sensor is used for in *vivo* measurement, it needs to function at body temperature, which is higher than the measurement temperature in our experiment. Therefore, the influence of temperature changes on the stability of sensor output is investigated as shown in Fig. 8. The left vertical axis represents the percentage ratio of the power change (P_1-P_0), which is defined as the output power at a specific temperature

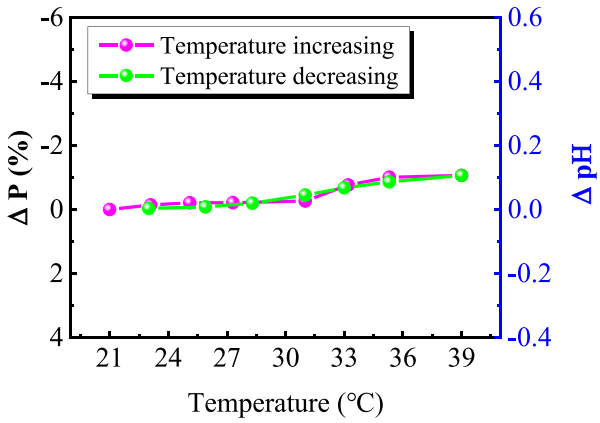

Fig. 8. Temperature response of U-shape sensor at a fixed pH (pH = 7).

(P_1) subtracted by the output power at 21°C (P_0), divided by P_0. The right vertical axis is the corresponding pH error attributed to the power variation. When the temperature is increased from 21 °C to 39 °C, the maximum interpreted pH change attributed to the power change is 0.12 pH. When the temperature decreases from 39 °C to 21 °C, the output power decreases as temperature decreases, which shows a repeatable measurement result. In addition, the pH response of the sensor at different temperatures is explored as shown in the supplementary file (Figure S.5). and the results show that when the temperature changes from 21 °C to 39 °C, the change in pH sensitivity is 0.01 dBm/pH which is 7% and 2.3% of its sensitivity for the pH range of 4.5–7.5 and 7.5–12.5, respectively.

D. Sensor Biocompatibility

It is extremely important to assess the biocompatibility of the sensor if it is to be used as part of a medical device interacting with a biological system. A full biocompatibility screen includes a range of tests such as Cytotoxicity, Sensitisation, Irritation / Intracutaneous Reactivity, Systemic Toxicity, Genotoxicity, Implantation and Hemocompatibility and is a time consuming and expensive process. An initial cytotoxicity test has therefore been conducted before a more extensive toxicological evaluation is performed. Cytotoxicity tests are designed to determine the toxicity to cells of compounds either qualitatively or quantitatively. Fig. 9 shows the cytotoxicity test results of sensing film via the two different methods (elution and direct contact) conducted in-house. The cytotoxicity is evaluated as:

$$Cytotoxicity(\%) = \frac{A_{sample} - A_{blank}}{A_{control} - A_{blank}} \times 100 \qquad (3)$$

where A_{sample} is the absorbance measurement from the sample (cells in contact with the tested film or its eluate), $A_{control}$ is absorbance from cells only and A_{blank} is the blank measurement. The toxicity percentages measured by the elution method and direct contact method at 24 & 72h are 96.36%, 83.9%, 79.35% and 92.34%, respectively, indicating that the proposed film is not considered cytotoxic according to the BS EN ISO 10993-12:2012 which defines cytotoxic as $< 70\%$.

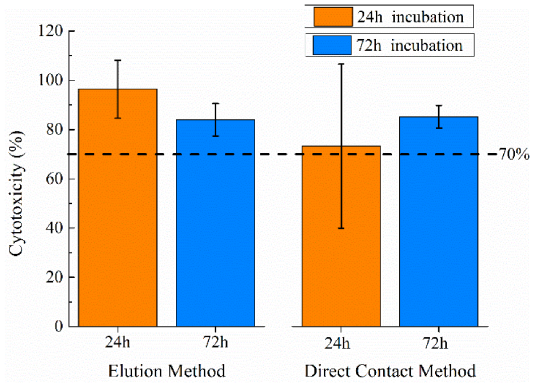

Fig. 9. Cytotoxicity as a percentage of the control for 24h &72h incubation with NIH 3T3 cells via the two methods (Elution and Direct contact).

TABLE I
A COMPARISON OF THE PROPOSED SENSOR TO SOME OTHER REPORTED DYE-FREE OFS PH SENSORS

Sensing film	Platform	pH range	Response time (t_r/t_f)	pH Resolution	Ref.
Hydrogel coating	Polymer FBG	4-8	114/180 s	0.027 pH	[37]
Polyaniline coating	tilted FBG	2–12	29/67 s	-	[17]
poly(ethylene glycol) diacrylate coating	polymer fiber Bragg grating	3-6.5	30 s	-	[16]
Hydrogel coating with a thin sliver film	SPR sensor based on MMF-SMF -MMF structure	1-12	12/24 s	-	[44]
Multiple layers of PAH/PAA bilayers	Cladding removed MMF tip	3-7	-	0.0022 pH	[38]
PANI- PVA composite layer	Cladding removed MMF tip	2–9	12/22 s	-	[39]
EC with sol-gel matrix	U-shape fiber	4.5-12.5	45/46 s	0.02 pH	This Paper

FBG: Fibre Bragg Grating, SPR: Surface Plasmon Resonance, PAH: poly (allylamine hydrochloride), PAA: poly(acrylic acid), PANI: Polyaniline, PVA: polyvinyl alcohol.

IV. DISCUSSION

Table I lists key sensing parameters of the proposed sensor in comparison to some other reported dye-free OFS pH sensors. Among these sensors, the proposed sensor shows a large detection range compared to the hydrogel coated FBG sensor [16], [37], PAH/PAA bilayers coated evanescent sensor [38] and PANI-PVA coated evanescent sensor [39]. It possesses a simple structure compared to FBG and SPR based sensors in terms of fabrication; it has a low temperature cross-sensitivity and does not require expensive wavelength interrogating devices. The test range and pH resolution of the proposed sensor are 4.5–12.5 and 0.02 pH respectively, satisfying the requirements of many biomedical applications. For example, normal skin has a pH

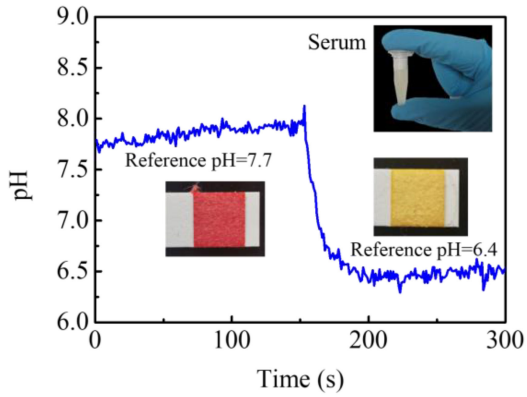

Fig. 10. Dynamic pH measurement of human serum with the OFS. The decrease of pH is introduced by titrating with HCL solution.

range of 4–6 and a wound typically has a pH range between 7 and 9 [40]. Most mammalian cells typically grow at pH 7.0–7.5 and a typical resolution for measuring the pH changes is 0.1 pH [41]. Whereas the pH of normal tissues is around 7.4, the extracellular pH of a tumour can range from 6.0 to 7.0 with a required resolution of 0.1 pH, which may have profound effects on cancer cell survival, somatic evolution, metastasis, and therapeutic response [42]. If an infant's recorded minimum pH value within 1 hour after birth is <7, acidosis may worsen the condition at birth potentially leading to death or cerebral palsy [43]. The resolution of the proposed sensor is 0.02 pH, which could be applied to the measurement of acidosis, although typically 0.01 is stated as ideal. At present the pH resolution is limited by the spectrometer resolution and a higher specification spectrometer could further improve resolution.

Although the refractive index of the pH sensing film under different pH solutions cannot be measured directly due to limitation of available instrumentation, we have eliminated the possibility of the change being due to a change in absorption of the coating. The absorption coefficient has been experimentally demonstrated to remain unchanged under different pH condition (Figure S.3). The experimentally observed results in pH sensing are consistent with a change in refractive index. The film is made of a solid silica matrix which prevents the swelling of the polymer inside of the film. The U-shape fibre was annealed under high temperature in which the stress was released, the radius is unlikely to change under different pH solution.

The measurement results of pH monitoring in human serum is shown in Fig. 10, which indicates that the proposed sensor is capable of monitoring the pH change in a biomedical environment while adjusting pH of the serum from about 7.7 to 6.4. The monitoring of pH in the range of 6–8 is important in biomedical applications, for example, when the infant's recorded minimum pH value within 1 hour after birth is <6.8, the probability of neonatal cerebral palsy or brain death will be as high as 21% [44]. A weak acid environment (pH = 6–7), which is common in solid tumor tissues, enhances the viability and invasion of tumor cells [45].

The sensor shows a change of pH with temperature of 0.12 over a wide temperature range (21–39°C) with the change much smaller over selected ranges such as body temperature (36.5–39°C). For many applications, temperature compensation will not be necessary; however, if required, temperature calibration can be conducted. Initial cytotoxicity tests indicate that the sensor is biocompatible, but for clinical implementation, a full biocompatibility procedure should be conducted.

The optical detection system used in this paper comprises CCD spectrometer and halogen light source would limit its use to a laboratory-based testing tool. As the measurement of pH actually relies on power change of single wavelength, the spectrometer and light source can therefore be replaced with a single LED and photodetector, which has been estimated to reduce cost to ~£15 [46]. As the sensor is based on power modulation it may suffer from light power drifting during continuous long-term monitoring. This can be overcome with a ratiometric method by introducing a reference photodetector intrinsically to monitor light stability and compensate drift.

V. Conclusion

A dye-free, U-shape optical fibre sensor coated with a silica-polymer composite film has been developed for the measurement of pH. pH is measured via a refractive index change of the film induced by pH as a result of changing aggregation of EC in a silica matrix. The sensor exhibits a pH detection range of 4.5 to 12.5. A linear response is obtained with a resolution of 0.02 pH within the pH range of 7.5–12.5. In addition, the proposed sensor is repeatable, has low hysteresis and exhibits low temperature cross-sensitivity in the tested range (21 °C to 39 °C). A non-cytotoxic feature of the sensing film tested with mouse fibroblast cells demonstrates the potential biocompatibility that is promising for in *vivo* application.

Acknowledgment

The authors would like to thank to Nanoscale and Microscale Research centre (nmRC) at the University of Nottingham for providing access to facilities.

References

[1] M. I. Khan, K. Mukherjee, R. Shoukat, and H. Dong, "A review on pH sensitive materials for sensors and detection methods," *Microsystem Technol.*, vol. 23, pp. 4391–4404, Oct. 2017.

[2] W. Huang, S. Deb, Y. Seo, S. Rao, M. Chiao, and J. C. Chiao, "A passive radio-frequency pH-sensing tag for wireless food-quality monitoring," *IEEE Sensors J.*, vol. 12, pp. 487–495, Mar. 2012.

[3] E. Prats-Alfonso, L. Abad, N. Casañ-Pastor, J. Gonzalo-Ruiz, and E. Baldrich, "Iridium oxide pH sensor for biomedical applications. Case urea–urease in real urine samples," *Biosensors Bioelectronics*, vol. 39, pp. 163–169, Jan. 2013.

[4] R. I. Freshney, in *Culture of Animal Cells: A Manual of Basic Technique and Specialized Applications*, Wiley, 2015.

[5] Y. Zhu *et al.*, "A multifunctional pro-healing zwitterionic hydrogel for simultaneous optical monitoring of pH and glucose in diabetic wound treatment," *Adv. Funct. Materials*, 2019, Art. no. 1905493.

[6] O. Thews and A. Riemann, "Tumor pH and metastasis: A malignant process beyond hypoxia," *Cancer Metastasis Rev.*, vol. 38, pp. 113–129, 2019.

[7] E. Allanson, T. Waqar, C. White, Ö. Tunçalp, and J. Dickinson, "Umbilical lactate as a measure of acidosis and predictor of neonatal risk: A systematic review," *BJOG: An Int. J. Obstet. Gynaecol.*, vol. 124, pp. 584–594, 2017.

[8] R. Correia, S. James, S. Lee, S. Morgan, and S. Korposh, "Biomedical application of optical fibre sensors," *J. Optics*, vol. 20, 2018, Art. no. 073003.

[9] D. Tosi, E. Schena, C. Molardi, and S. Korganbayev, "Fiber optic sensors for sub-centimeter spatially resolved measurements: Review and biomedical applications," *Opt. Fiber Technol.*, vol. 43, pp. 6–19, 2018.

[10] D. Tosi, S. Poeggel, I. Iordachita, and E. Schena, "Fiber optic sensors for biomedical applications," in *Opto-Mechanical Fiber Optic Sensors*, ed: Elsevier, Amsterdam, The Netherlands; New York, 2018, pp. 301–333.

[11] V. Moradi, M. Akbari, and P. Wild, "A fluorescence-based pH sensor with microfluidic mixing and fiber optic detection for wide range pH measurements," *Sensors Actuators A: Phys.*, vol. 297, 2019, Art. no. 111507.

[12] S. Islam *et al.*, "Surface functionality and optical properties impact of phenol red dye on mesoporous silica matrix for fiber optic pH sensing," *Sensors Actuators A: Phys.*, vol. 276, pp. 267–277, 2018.

[13] H. M. R. Gonçalves, C. D. Maule, P. A. S. Jorge, and J. C. G. Esteves da Silva, "Fiber optic lifetime pH sensing based on ruthenium(II) complexes with dicarboxybipyridine," *Analytica Chimica Acta*, vol. 626, pp. 62–70, Sep. 2008.

[14] M. Chauhan and V. K. Singh, "Fiber optic pH sensor using tio2-sio2 composite layer with a temperature cross-sensitivity feature," *Optik*, vol. 212, Jun. 2020, Art. no. 164709.

[15] T. M. Butler, B. D. MacCraith, and C. McDonagh, "Leaching in sol–gel-derived silica films for optical pH sensing," *J. Non-Crystalline Solids*, vol. 224, pp. 249–258, Apr. 1998.

[16] X. Cheng, J. Bonefacino, B. Guan, and H. Tam, "All-polymer fiber-optic pH sensor," *Optics express*, vol. 26, pp. 14610–14616, 2018.

[17] A. L. Aldaba, Á. González-Vila, M. Debliquy, M. Lopez-Amo, C. Caucheteur, and D. Lahem, "Polyaniline-coated tilted fiber bragg gratings for pH sensing," *Sensors Actuators B: Chem.*, vol. 254, pp. 1087–1093, 2018.

[18] V. Semwal and B. D. Gupta, "Highly sensitive surface plasmon resonance based fiber optic pH sensor utilizing rGO-Pani nanocomposite prepared by in situ method," *Sensors Actuators B: Chem.*, vol. 283, pp. 632–642, Mar. 2019.

[19] S. A. Shahamirifard, M. Ghaedi, and S. Hajati, "A new silver (I) ions optical sensor based on nanoporous thin films of sol–gel by rose bengal dye," *Sensors Actuators B: Chem.*, vol. 259, pp. 20–29, Apr. 2018.

[20] N. M. El-Ashgar, A. I. El-Basioni, I. M. El-Nahhal, S. M. Zourob, T. M. El-Agez, and S. A. Taya, "Sol-gel thin films immobilized with bromocresol purple pH-sensitive indicator in presence of surfactants," *ISRN Analytical Chem.*, vol. 2012, 2012.

[21] C. J. Brinker and G. W. Scherer, in *Sol-gel Science: The physics and Chemistry of Sol-Gel Processing*, Academic, New York; Orlando, FL; San Diego, CA, 2013.

[22] J. Rayss and G. Sudolski, "Ion adsorption in the porous sol–gel silica layer in the fibre optic pH sensor," *Sensors Actuators B: Chem.*, vol. 87, pp. 397–405, 2002.

[23] M. El-Sakhawy, S. Kamel, A. Salama, and H.-A. Sarhan, "Carboxymethyl cellulose acetate butyrate: A review of the preparations, properties, and applications," *J. Drug Del.*, vol. 2014, Dec. 2014, Art. no. 575969.

[24] S. Rajesh, K. H. Shobana, S. Anitharaj, and D. R. Mohan, "Preparation, morphology, performance, and hydrophilicity studies of poly(amide-imide) incorporated cellulose acetate ultrafiltration membranes," *Ind. Eng. Chem. Res.*, vol. 50, pp. 5550–5564, May 2011.

[25] S. Mun, Y. Chen, and J. Kim, "Cellulose–titanium dioxide–multiwalled carbon nanotube hybrid nanocomposite and its ammonia gas sensing properties at room temperature," *Sensors Actuators B: Chem.*, vol. 171–172, pp. 1186–1191, Aug. 2012.

[26] M. Salmani, G. K. G. H. Rounaghi, and M. Chamsaz, "An optical sensor for determination of low pH values based on covalent immobilization of congo red on triacetyl cellulose films via epichlorohydrin," *Sensors Actuators B: Chem.*, vol. 254, pp. 177–181, Jan. 2018.

[27] C.-S. Chu and C.-J. Su, "Fluorescence ratiometric optical broad range pH sensor based on CdSe/ZnS quantum dots and O170 embedded in ethyl cellulose matrix," *J. Lightw. Technol.*, vol. 36, pp. 857–862, 2018.

[28] B. Gupta and N. K. Sharma, "Fabrication and characterization of U-shaped fiber-optic pH probes," *Sensors Actuators B: Chem.*, vol. 82, pp. 89–93, 2002.

[29] A. Pathak and V. Singh, "U shaped fiber-optic pH sensor using Sol-gel coating over TiO2," *Frontiers Optics*, 2017, Art. no. JTu2A. 51.

[30] B. Lindman, B. Medronho, L. Alves, C. Costa, H. Edlund, and M. Norgren, "The relevance of structural features of cellulose and its interactions to dissolution, regeneration, gelation and plasticization phenomena," *Phys. Chem. Chem. Physics*, vol. 19, pp. 23704–23718, 2017.

[31] M. Remouche, F. Georges, and P. Meyrueis, "Flexible optical waveguide bent loss attenuation effects analysis and modeling application to an intrinsic optical fiber temperature sensor," 2012.

[32] V. Ruddy, B. MacCraith, and J. Murphy, "Evanescent wave absorption spectroscopy using multimode fibers," *J. Applied Phys.*, vol. 67, pp. 6070–6074, 1990.

[33] C. G. Danny, M. D. Raj, and V. Sai, "Investigating the refractive index sensitivity of U-bent fiber optic sensors using ray optics," *J. Lightw. Technol.*, vol. 38, pp. 1580–1588, 2020.

[34] J. Liu, Y. Chen, Y. Li, H. Zhang, S. Zheng, and S. Xu, "Switchable dual-wavelength Q-switched fiber laser using multilayer black phosphorus as a saturable absorber," *Photon. Res.*, vol. 6, pp. 198–203, Mar. 2018.

[35] Y. Bao and G. Chen, "High-temperature measurement with brillouin optical time domain analysis of an annealed fused-silica single-mode fiber," *Optics Lett.*, vol. 41, pp. 3177–3180, 2016.

[36] M. Sulpizi, M.-P. Gaigeot, and M. Sprik, "The silica–water interface: How the silanols determine the surface acidity and modulate the water properties," *J. Chem. Theory Comput.*, vol. 8, pp. 1037–1047, Mar. 2012.

[37] J. Janting, J. K. M. Pedersen, G. Woyessa, K. Nielsen, and O. Bang, "Small and robust all-polymer fiber bragg grating based pH sensor," *J. Lightw. Technol.*, vol. 37, pp. 4480–4486, Sep. 2019.

[38] K. Mohd Yatim, G. Krishnan, H. Bakhtiar, S. Daud, and S. Wadi Harun, "The pH sensor based optical fiber coated with PAH/PAA," *J. Phys.: Conf. Ser.*, vol. 1371, Nov. 2019, Art. no. 012021.

[39] T. Khanikar and V. K. Singh, "PANI-PVA composite film coated optical fiber probe as a stable and highly sensitive pH sensor," *Optical Materials*, vol. 88, pp. 244–251, Feb. 2019.

[40] A. Tamayol *et al.*, "Flexible pH-Sensing hydrogel fibers for epidermal applications," *Adv. Healthcare Materials*, vol. 5, pp. 711–719, Mar. 2016.

[41] D. Kattipparambil Rajan *et al.*, "Optical non-contact pH measurement in cell culture with sterilizable, modular parts," *Talanta*, vol. 161, pp. 755–761, Dec. 2016.

[42] C. R. Justus and L. V. Yang, "GPR4 decreases B16F10 melanoma cell spreading and regulates focal adhesion dynamics through the G13/Rho signaling pathway," *Exp. Cell Res.*, vol. 334, pp. 100–113, May 2015.

[43] R. Kelly *et al.*, "Dose-dependent relationship between acidosis at birth and likelihood of death or cerebral palsy," *Archives Dis. Childhood-Fetal Neonatal Edition*, vol. 103, pp. F567–F572, 2018.

[44] A. Arifin Hardianti, M. Yunus, and S. Dewang, "Application of plastic optical fiber material as pH measurement sensor using loop configuration," *J. Phys.: Conf. Ser.*, vol. 1317, Oct. 2019, Art no. 012047.

[45] W. Li, Y. Zhou, C. Shang, H. Sang, and H. Zhu, "Effects of environmental pH on the growth of gastric cancer cells," *Gastroenterol. Res. Pract.*, vol. 2020, 2020.

[46] C. He *et al.*, "Real-time humidity measurement during sports activity using optical fibre sensing," *Sensors*, vol. 20, 2020, Art. no. 1904.